

## An All-Metal Aromatic Sandwich Complex $[Sb_3Au_3Sb_3]^{3-}$

Fu-Xing Pan,<sup>†,§,#</sup> Lei-Jiao Li,<sup>†,#</sup> Ying-Jin Wang,<sup>‡</sup> Jin-Chang Guo,<sup>‡</sup> Hua-Jin Zhai,<sup>\*,‡,||</sup> Li Xu,<sup>†</sup> and Zhong-Ming Sun<sup>\*,†,‡</sup>

<sup>†</sup>State Key Laboratory of Rare Earth Resource Utilization, Changchun Institute of Applied Chemistry, Chinese Academy of Sciences, Changchun, Jilin 130022, China

<sup>‡</sup>Nanocluster Laboratory, Institute of Molecular Science and <sup>||</sup>State Key Laboratory of Quantum Optics and Quantum Optics Devices, Shanxi University, Taiyuan 030006, China

<sup>§</sup>University of Chinese Academy of Sciences, Beijing 100049, China

<sup>\*</sup>State Key Laboratory of Structural Chemistry, Fujian Institute of Research on the Structure of Matter, Chinese Academy of Sciences, Fuzhou, Fujian 350002, China

### S Supporting Information

**ABSTRACT:** A sandwich complex, as exemplified by ferrocene in the 1950s, usually refers to one metal center bound by two arene ligands. The subject has subsequently been extended to carbon-free aromatic ligands and multiple-metal-atom “monolayered” center, but not to an all-metal species. Here, we describe the synthesis of an unprecedented all-metal aromatic sandwich complex,  $[Sb_3Au_3Sb_3]^{3-}$ , which was isolated as  $K([2.2.2]\text{crypt})^+$  salt and identified by single-crystal X-ray diffraction. Quantum chemical calculations indicate that intramolecular electron transfers for the three metallic layers ( $\text{Sb} \rightarrow \text{Au}$  donation and  $\text{Sb} \leftarrow \text{Au}$  back-donation) markedly redistribute the valence electrons from the *cyclo*- $\text{Sb}_3$  ligands and  $\text{Au}_3$  interlayer to the  $\text{Au}-\text{Sb}$  bonds, which hold the complex together via  $\sigma$  bonding. Each *cyclo*- $\text{Sb}_3$  possesses aromaticity with delocalized three-center three-electron (3c-3e)  $\pi$  bonds, which are essentially equivalent to a 3c-4e  $\pi\pi^*$  triplet system, following the reversed 4n Hückel rule for aromaticity in a triplet state.

The first sandwich complex  $(\text{C}_5\text{H}_5)_2\text{Fe}$ , termed “ferrocene”,<sup>1,2</sup> has sprouted new research disciplines in chemistry and materials science and precipitated tremendous applications in chemical synthesis, catalysis, and material precursors.<sup>3</sup> In 2002, a carbon-free sandwich complex  $[(\text{P}_5)_2\text{Ti}]^{2-}$  was reported, and shortly after that the interlayer was extended from mononuclear metal center to multiple metal atoms.<sup>4-8</sup> These relatively recent findings have expanded the structural concept of sandwich complexes and represent new horizons for materials research. However, an all-metal sandwich complex, in which a metal center or metal sheet is jammed between two aromatic metal rings, has not been isolated, although a large amount of molecules such as  $[\text{Al}_4\text{TiAl}_4]^{2-}$ ,  $[\text{Sb}_4\text{FeSb}_4]^{2-}$ , and  $[\text{Sb}_5\text{TiSb}_5]^{2-}$  has been theoretically proposed, following the discovery of aromatic  $\text{Al}_4^{2-}$  and  $[(\text{P}_5)_2\text{Ti}]^{2-}$  complexes.<sup>9-16</sup> On the other hand, triggered by the abundance of the triangular Au complexes, sandwich compounds such as  $[\text{c-Au}_3(\mu_2-\text{Cl})_3](\text{C}_6\text{H}_6)_2$  and  $[\text{c-Au}_3(\mu_2-\text{Cl})_3](\text{B}_3\text{N}_3\text{H}_6)_2$  have also been predicted theoretically.<sup>17</sup> The aforementioned remarkable works have inspired us to explore the possibility to synthesize the all-metal aromatic sandwich complexes. Here we

describe the synthesis and characterization of an entirely new cluster anion,  $[Sb_3Au_3Sb_3]^{3-}$ , in which an  $\text{Au}_3$  ring is sandwiched by two *cyclo*- $\text{Sb}_3$ .

The  $[Sb_3Au_3Sb_3]^{3-}$  complex, crystallized in the form of  $[\text{K}([2.2.2]\text{crypt})]_3[Sb_3Au_3Sb_3]\cdot(0.5\text{PPh}_3)\cdot\text{en}$  (**1**; en = ethylenediamine), was isolated by introducing  $\text{Au}(\text{PPh}_3)\text{Ph}$  into the ethylenediamine solution of  $\text{K}_5\text{Sb}_4$  and  $[2.2.2]\text{crypt}$ . After recrystallization in pyridine (py), **1** could transform to  $[\text{K}([2.2.2]\text{crypt})]_3[Sb_3Au_3Sb_3]\cdot3\text{py}$  (**2**). The prismatic anion  $[Sb_3Au_3Sb_3]^{3-}$  has pseudo- $D_{3h}$  symmetry (Figure 1). To our knowledge, such a ligand-free triangular prismatic structure has never been reported. Furthermore,  $[Sb_3Au_3Sb_3]^{3-}$  appears to be the first all-metal aromatic sandwich complex, in which a monolayered metal sheet is jammed between two metallic, aromatic ligands. In the following, only the data of **1** will be presented and discussed.

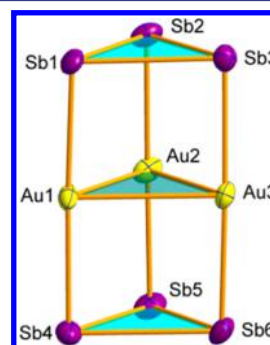


**Figure 1.** Thermal ellipsoid plot of the molecular cluster anion  $[Sb_3Au_3Sb_3]^{3-}$  (drawn at 50% probability). Selected bond distances (angstroms) and angles (degrees):  $\text{Au1}-\text{Au2}$ , 2.9404(6);  $\text{Au1}-\text{Au3}$ , 2.9536(6);  $\text{Au2}-\text{Au3}$ , 2.7179(7);  $\text{Au1}-\text{Sb1}$ , 2.6093(9);  $\text{Au1}-\text{Sb4}$ , 2.5998(10);  $\text{Au2}-\text{Sb2}$ , 2.5992(9);  $\text{Au2}-\text{Sb5}$ , 2.5992(9);  $\text{Au3}-\text{Sb3}$ , 2.5919(9);  $\text{Au3}-\text{Sb6}$ , 2.5939(10);  $\text{Sb1}-\text{Sb2}$ , 2.8615(10);  $\text{Sb1}-\text{Sb3}$ , 2.8708(10);  $\text{Sb2}-\text{Sb3}$ , 2.8489(11);  $\text{Sb4}-\text{Sb5}$ , 2.8648(11);  $\text{Sb4}-\text{Sb6}$ , 2.8619(12);  $\text{Sb5}-\text{Sb6}$ , 2.8824(13);  $\text{Au2}-\text{Au1}-\text{Au3}$ , 59.346(15);  $\text{Au2}-\text{Au3}-\text{Au1}$ , 60.101(14);  $\text{Sb2}-\text{Sb1}-\text{Sb3}$ , 59.60(3);  $\text{Sb2}-\text{Sb3}-\text{Sb1}$ , 60.04(3);  $\text{Sb4}-\text{Sb5}-\text{Sb6}$ , 59.73(3);  $\text{Sb4}-\text{Sb6}-\text{Sb5}$ , 59.83(3).

Received: July 23, 2015

Published: August 14, 2015

In  $[\text{Sb}_3\text{Au}_3\text{Sb}_3]^{3-}$  complex, the bond distances of Au–Au (2.918 to 2.954 Å) are confined in a very narrow range (as compared with 2.900 to 3.095 Å in  $[\text{Au}_3\text{Ge}_{18}]^{5-}$ ),<sup>18a</sup> which are slightly longer than those in typical gold clusters<sup>19</sup> but shorter than those in the  $\text{Au}_3$  rings of  $[(\text{LAu})_6(\text{N}_2)]^{2+}$  (3.244 Å in average; L = PPh<sub>2</sub>iPr).<sup>18b</sup> Other transition-metal triangles flanked by aromatic arenes were only observed in sandwich complex  $[\text{Pd}_3(\text{C}_7\text{H}_7)_2\text{Cl}_3]^-$  and related derivatives.<sup>5-7,20-24</sup> However, notable differences set  $\text{Au}_3$  apart from  $\text{Pd}_3$ , because the  $[\text{Pd}_3(\text{C}_7\text{H}_7)_2]^{2+}$  core is less stable without the substituents. The Au–Sb distances (2.592 to 2.609 Å) are almost equal with each other, which are markedly shorter than those in complexes (1,8-naphthalene-diyl)<sub>2</sub>(Ph<sub>2</sub>Sb)Au (2.762 Å in average) and  $[^7\text{Bu}_4\text{N}]^+[(1,8\text{-naphthalene-diyl})_2(\text{Ph}_2\text{SbF})\text{Au}]$  (2.771 Å in average),<sup>25</sup> implying strong Au–Sb interactions in  $[\text{Sb}_3\text{Au}_3\text{Sb}_3]^{3-}$ . The three Sb–Au–Sb angles are close to 180° (177.87 to 178.15°). As a consequence, Au exhibits linear coordination, and the three metallic layers are virtually coplanar (dihedral angles: 0.08 to 0.39°).

The Sb–Sb distances also span a narrow range within  $\pm 0.017$  Å (2.849 to 2.882 Å). The  $\text{Sb}_3$  units are almost equilateral triangles (59.60 to 60.44°) and bind or accommodate the  $\text{Au}_3$  ring favorably via Au–Sb interactions; see below for bonding analysis. The *cyclo*-Sb<sub>3</sub> in  $[\text{Sb}_3\text{Au}_3\text{Sb}_3]^{3-}$  also serves as new evidence for the existence of Sb<sub>3</sub><sup>3-</sup> fragment upon dissolving K<sub>3</sub>Sb<sub>4</sub> in solvents, which has been put forward for more than 80 years.<sup>26</sup> As predicted by Hagelberg et al.,<sup>27</sup> the *cyclo*-Sb<sub>3</sub><sup>3-</sup> is less-preferred compared with the bent ozone style, which was confirmed by Sevov in experiments.<sup>28</sup> Our results indicate that the *cyclo*-Sb<sub>3</sub> species can be successfully stabilized by the  $\text{Au}_3$  ring.

To gain insight into the bonding nature of  $[\text{Sb}_3\text{Au}_3\text{Sb}_3]^{3-}$ , we have performed quantum chemical calculations at density-functional theory (DFT) level using Gaussian 09 program;<sup>29</sup> see Supporting Information for details. The DFT calculations show that the optimized structure of  $[\text{Sb}_3\text{Au}_3\text{Sb}_3]^{3-}$  features an ideal  $D_{3h}$  symmetry. The HOMO-LUMO energy gap is calculated to be 3.08 eV, which is surprisingly large in particular for an all-metal complex.  $[\text{Sb}_3\text{Au}_3\text{Sb}_3]^{3-}$  possesses nondeltahedral architecture, and thus it no longer follows the conventional Wade's rules.<sup>30</sup> Alternatively, the Sb and Au atoms contribute 18 and 3 valence electrons, respectively, for chemical bonding in the complex (the Sb 5s and Au 5d lone-pairs not included). These 21 electrons in addition to the 3 charges for the overall cluster amount to a total of 24 electrons, which are insufficient for the formation of 15 two-center two-electron (2c-2e) bonds in the triple-layered triangular prism structure (Figure 1). However, the mismatch can be partially offset due to the low bond order for the three Au–Au bonds. The calculated Wiberg bond order<sup>31</sup> of Au–Au is 0.32, which is much smaller than those of Au–Sb (1.09) and Sb–Sb (1.21). Thus,  $[\text{Sb}_3\text{Au}_3\text{Sb}_3]^{3-}$  shows relatively weak Au–Au interactions, including aurophilicity as noted by earlier researches.<sup>32-35</sup> By definition, aurophilicity describes the closed-shell interactions between two Au(I) d<sup>10</sup> centers at the “magic” distance of ~3 Å, which are of dispersive nature but substantially enhanced in gold due to relativistic effects, comparable in strength to typical hydrogen bonds. In  $[\text{Sb}_3\text{Au}_3\text{Sb}_3]^{3-}$ , the Au centers are not in the Au(I) state, but the Au 6s electrons appear to participate negligibly in Au–Au bonding; see below. According to the latest recommended covalent radii by Pyykkö,<sup>36,37</sup> typical distances for the Au–Au, Sb–Sb, and Au–Sb single bonds are 2.48, 2.80, and 2.64 Å, respectively. The observed bond distances in  $[\text{Sb}_3\text{Au}_3\text{Sb}_3]^{3-}$  are entirely consistent with the calculated Wiberg bond orders.

The potential energy surface of Sb<sub>3</sub><sup>3-</sup> is known to possess two clear minima, representing two Sb<sub>3</sub><sup>3-</sup> species with an equilateral triangle structure and a bent one, respectively.<sup>27</sup> Similar to the isoelectronic ozone molecule, the *cyclo*-Sb<sub>3</sub><sup>3-</sup> is less stable than the bent counterpart ( $\Delta E = 0.5$  eV). Nevertheless, the two *cyclo*-Sb<sub>3</sub> in  $[\text{Sb}_3\text{Au}_3\text{Sb}_3]^{3-}$  (Figure 1) are equilateral triangles with  $D_{3h}$  symmetry, hinting that these Sb<sub>3</sub> ligands are not in Sb<sub>3</sub><sup>3-</sup> charge state. Intramolecular electron transfer occurs between Sb<sub>3</sub> and  $\text{Au}_3$  in the present  $[\text{Sb}_3\text{Au}_3\text{Sb}_3]^{3-}$  cluster, where the two Sb<sub>3</sub> serve as electron donors and the  $\text{Au}_3$  ring as an acceptor. In effect, the two Sb<sub>3</sub> ligands collectively donate three electrons to  $\text{Au}_3$ , so that three Au 6s based molecular orbitals (MOs) in the latter are occupied (HOMO-15 and HOMO-2/HOMO-2'; Figure 2B).<sup>38</sup>

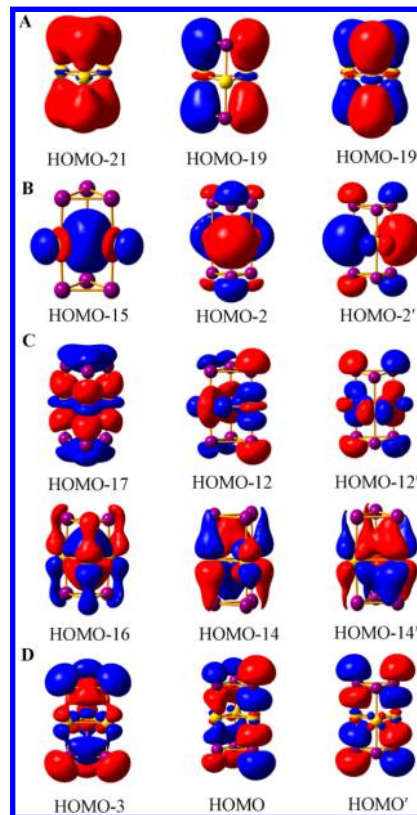


**Figure 2.** Plots of some key occupied MOs of  $[\text{Sb}_3\text{Au}_3\text{Sb}_3]^{3-}$  cluster, generated by GaussView (Sb: purple, Au: yellow).<sup>38</sup> (A) Sb → Au donation: HOMO-21 and HOMO-19/HOMO-19'. (B) Au 6s based MOs: HOMO-15 and HOMO-2/HOMO-2'. The latter two are responsible for Sb → Au donation of 3 electrons. (C) Au → Sb back-donation: HOMO-17, HOMO-12/HOMO-12', HOMO-16, and HOMO-14/HOMO-14'. (D) Globally delocalized three-center three-electron (3c-3e) bonds in the two *cyclo*-Sb<sub>3</sub>: HOMO-3 and HOMO/HOMO'. All these 15 MOs (except HOMO-15) collectively contribute to Au–Sb bonding in  $[\text{Sb}_3\text{Au}_3\text{Sb}_3]^{3-}$ .

However, complex donation/back-donation processes (Figure 2) drastically redistribute the electrons from three Sb<sub>3</sub> and  $\text{Au}_3$  monolayers to six Au–Sb edges, resulting in substantial Au–Sb bonding while reducing the Sb–Sb and Au–Au bond orders. Considering the large electronegativity of Sb, the Au–Sb interaction should be primarily considered as covalent.<sup>39</sup>

To be quantitative, we implement the charge decomposition analysis (CDA; see Table S4).<sup>40</sup> The CDA results show that electron donation and back-donation indeed exist between two *cyclo*-Sb<sub>3</sub> ligands and the  $\text{Au}_3$  ring. Specifically, 0.937 e is donated from Sb<sub>3</sub> to  $\text{Au}_3$ , while 0.241 e is back-donated from  $\text{Au}_3$  to Sb<sub>3</sub>,

resulting in weakened Jahn–Teller effect in *cyclo-Sb<sub>3</sub>* with respect to gas-phase Sb<sub>3</sub><sup>3-</sup> species. According to the CDA, HOMO-21 and HOMO-19/HOMO-19' contribute partially to electron donation from Sb<sub>3</sub> to Au<sub>3</sub>, whereas HOMO-2/HOMO-2' represent the major donation from Sb<sub>3</sub> to Au<sub>3</sub> (formally by three electrons in total; Figure 2B). On the other hand, HOMO-17, HOMO-16, and relevant MOs contribute to electron back-donation from Au<sub>3</sub> to Sb<sub>3</sub> (Figure 2C). The above 12 MOs distinctly indicate that Au–Sb bonding is covalent in nature, although it is not an equal sharing. It is remarkable that, although not one 2c-2e Au–Sb bond can be identified from the MOs, the donation and back-donation from over 10 MOs (Figure 2) manage to “make” six such bonds, as revealed from the Wiberg bond order and the Au–Sb distances. Donation and back-donation are favorable for covalent bonding, in which the matched electronegativity between the Au and Sb elements should play a pivotal role.

Interestingly, HOMO/HOMO' and HOMO-3 show delocalized  $\pi$  characters, which are primarily based on two *cyclo-Sb<sub>3</sub>* ligands (Figure 2D). HOMO and HOMO' are doubly degenerate. Orbital analyses show that HOMO is composed of 90.7% Sb 5p and 9.3% Au 6p, whereas HOMO' is made up of 95.1% Sb 5p along with 4.9% Au 6p. The components of HOMO-3 include 95.9% Sb 5p and 2.5% Au 6p, with an additional 1.6% Au 5d. In short, the three MOs are primarily derived from Sb 5p atomic orbitals. These  $\pi$  MOs are globally delocalized within two *cyclo-Sb<sub>3</sub>*, collectively carrying the three extra charges for the complex. Thus, each *cyclo-Sb<sub>3</sub>* has a formal charge state of Sb<sub>3</sub><sup>1.5-</sup>. This exactly offsets the Sb  $\rightarrow$  Au  $\sigma$  donation (three electrons in total for two Sb<sub>3</sub>; Figure 2B), maintaining each *cyclo-Sb<sub>3</sub>* ligand a system with 15 valence electrons (including Sb 5s lone-pairs).<sup>41</sup> The consequence of the bonding pattern is that each Sb<sub>3</sub> effectively has a set of delocalized three-center three-electron (3c-3e)  $\pi$  bonds (Figure 2D). Note that the 3c-3e  $\pi$  bonds are basically equivalent to a typical 3c-4e  $\pi\pi^*$  triplet system,<sup>13,42</sup> except that in the former the completely bonding MO and the degenerate, partially bonding MOs are all half-occupied, whereas in a 3c-4e  $\pi\pi^*$  triplet system the completely bonding MO is fully occupied. A 3c-4e  $\pi\pi^*$  triplet system is known to be aromatic due to the reversed 4n Hückel rule for aromaticity in a triplet state,<sup>42</sup> thus the [Sb<sub>3</sub>Au<sub>3</sub>Sb<sub>3</sub>]<sup>3-</sup> cluster with two 3c-3e  $\pi$  *cyclo-Sb<sub>3</sub>* ligands is  $\pi$  aromatic.<sup>43–45</sup> So far the nucleus-independent chemical shift (NICS) is an efficient probe for aromaticity.<sup>46,47</sup> The calculated NICS(1)<sub>zz</sub> is -23.13 ppm for each *cyclo-Sb<sub>3</sub>* in [Sb<sub>3</sub>Au<sub>3</sub>Sb<sub>3</sub>]<sup>3-</sup>, consistent with strong  $\pi$  aromaticity for this unique triangular prism cluster. For comparison, NICS(1)<sub>zz</sub> for benzene is -29.87 ppm at the same level of theory. The above analysis offers new insight for the bonding nature in Au–Sb clusters. We also anticipate that the present all-metal, aromatic sandwich Au–Sb cluster may pave the way for syntheses of entirely new classes of sandwich complexes and find potential technological applications.

## ASSOCIATED CONTENT

### Supporting Information

The Supporting Information is available free of charge on the ACS Publications website at DOI: [10.1021/jacs.5b07730](https://doi.org/10.1021/jacs.5b07730).

X-ray crystallographic data ([CIF](#))

Experimental details, selected bond lengths and angles, details on energy-dispersive X-ray and DFT calculations ([PDF](#))

## AUTHOR INFORMATION

### Corresponding Authors

\*[szm@ciac.ac.cn](mailto:szm@ciac.ac.cn)

\*[hj.zhai@sxu.edu.cn](mailto:hj.zhai@sxu.edu.cn)

### Author Contributions

#These authors contributed equally.

### Notes

The authors declare no competing financial interest.

## ACKNOWLEDGMENTS

We thank Dr. Xue-Bin Wang and Dr. Jun Li for valuable discussion. This work was supported by the National Natural Science Foundation of China (21171162) and the State Key Laboratory of Quantum Optics and Quantum Optics Devices (KF201402). H.J.Z. gratefully acknowledges the start-up fund from Shanxi University for support.

## REFERENCES

- Wilkinson, G.; Rosenblum, M.; Whiting, M. C.; Woodward, R. B. *J. Am. Chem. Soc.* **1952**, *74*, 2125–2126.
- Fischer, E. O.; Pfab, W. Z. *Naturforsch., B: J. Chem. Sci.* **1952**, *7*, 377–379.
- Togni, A.; Halterman, R. L.; Eds. *Metallocenes: Synthesis Reactivity Applications*; Wiley-VCH, Weinheim, Germany, 1998.
- Urnéžius, E.; Brennessel, W. W.; Cramer, C. J.; Ellis, J. E.; Schleyer, P. v. R. *Science* **2002**, *295*, 832–834.
- Murahashi, T.; Fujimoto, M.; Oka, M.; Hashimoto, Y.; Uemura, T.; Tatsumi, Y.; Nakao, Y.; Ikeda, A.; Sakaki, S.; Kurosawa, H. *Science* **2006**, *313*, 1104–1107.
- Murahashi, T.; Fujimoto, M.; Kawabata, Y.; Inoue, R.; Ogoshi, S.; Kurosawa, H. *Angew. Chem., Int. Ed.* **2007**, *46*, 5440–5443.
- (a) Murahashi, T.; Hashimoto, Y.; Chiyoda, K.; Fujimoto, M.; Uemura, T.; Inoue, R.; Ogoshi, S.; Kurosawa, H. *J. Am. Chem. Soc.* **2008**, *130*, 8586–8587. (b) Murahashi, T.; Usui, K.; Inoue, R.; Ogoshi, S.; Kurosawa, H. *Chem. Sci.* **2011**, *2*, 117–122.
- (a) Tatsumi, Y.; Shirato, K.; Murahashi, T.; Ogoshi, S.; Kurosawa, H. *Angew. Chem., Int. Ed.* **2006**, *45*, 5799–5803. (b) Murahashi, T.; Kato, N.; Uemura, T.; Kurosawa, H. *Angew. Chem., Int. Ed.* **2007**, *46*, 3509–3512. (c) Tatsumi, Y.; Murahashi, T.; Okada, M.; Ogoshi, S.; Kurosawa, H. *Chem. Commun.* **2008**, 477–479. (d) Murahashi, T.; Mino, Y.; Chiyoda, K.; Ogoshi, S.; Kurosawa, H. *Chem. Commun.* **2008**, 4061–4063. (e) Murahashi, T.; Inoue, R.; Usui, K.; Ogoshi, S. *J. Am. Chem. Soc.* **2009**, *131*, 9888–9889. (f) Murahashi, T.; Takase, K.; Oka, M.; Ogoshi, S. *J. Am. Chem. Soc.* **2011**, *133*, 14908–14911. (g) Murahashi, T.; Shirato, K.; Fukushima, A.; Takase, K.; Suenobu, T.; Fukuzumi, S.; Ogoshi, S.; Kurosawa, H. *Nat. Chem.* **2012**, *4*, 52–58. (h) Murahashi, T.; Kimura, S.; Takase, K.; Ogoshi, S.; Yamamoto, K. *Chem. Commun.* **2013**, *49*, 4310–4312. (i) Murahashi, T.; Takase, K.; Usui, K.; Kimura, S.; Fujimoto, M.; Uemura, T.; Ogoshi, S.; Yamamoto, K. *Dalton Trans.* **2013**, *42*, 10626–10632. (j) Horiuchi, S.; Tachibana, Y.; Yamashita, M.; Yamamoto, K.; Masai, K.; Takase, K.; Matsutani, T.; Kawamata, S.; Kurashige, Y.; Yanai, T.; Murahashi, T. *Nat. Commun.* **2015**, *6*, doi: [10.1038/ncomms7742](https://doi.org/10.1038/ncomms7742).
- Li, X.; Kuznetsov, A. E.; Zhang, H. F.; Boldyrev, A. I.; Wang, L. S. *Science* **2001**, *291*, 859–861.
- Mercero, J. M.; Ugalde, J. M. *J. Am. Chem. Soc.* **2004**, *126*, 3380–3381.
- Mercero, J. M.; Formoso, E.; Matxain, J. M.; Eriksson, L. A.; Ugalde, J. M. *Chem. - Eur. J.* **2006**, *12*, 4495–4502.
- Li, X.; Zhang, H. F.; Wang, L. S.; Kuznetsov, A. E.; Cannon, N. A.; Boldyrev, A. I. *Angew. Chem., Int. Ed.* **2001**, *40*, 1867–1870.
- Boldyrev, A. I.; Wang, L. S. *Chem. Rev.* **2005**, *105*, 3716–3757.
- Li, Z.; Wu, W.; Li, S. *J. Mol. Struct.: THEOCHEM* **2009**, *908*, 73–78.
- Maslowsky, E. *Coord. Chem. Rev.* **2011**, *255*, 2746–2763.

- (16) Lein, M.; Frunzke, J.; Frenking, G. *Inorg. Chem.* **2003**, *42*, 2504–2511.
- (17) Tsipis, A. C.; Stalikas, A. V. *Inorg. Chem.* **2013**, *52*, 1047–1060.
- (18) (a) Spiekermann, A.; Hoffmann, S. D.; Kraus, F.; Fässler, T. F. *Angew. Chem., Int. Ed.* **2007**, *46*, 1638–1640. (b) Shan, H.; Yang, Y.; James, A. J.; Sharp, P. R. *Science* **1997**, *275*, 1460–1462.
- (19) Konishi, K. *Struct. Bonding (Berlin)* **2014**, *161*, 49–86.
- (20) Murahashi, T.; Usui, K.; Tachibana, Y.; Kimura, S.; Ogoshi, S. *Chem. - Eur. J.* **2012**, *18*, 8886–8890.
- (21) Murahashi, T.; Kimura, S.; Takase, K.; Uemura, T.; Ogoshi, S.; Yamamoto, K. *Chem. Commun.* **2014**, *50*, 820–822.
- (22) Ishikawa, Y.; Kimura, S.; Takase, K.; Yamamoto, K.; Kurashige, Y.; Yanai, T.; Murahashi, T. *Angew. Chem., Int. Ed.* **2015**, *54*, 2482–2486.
- (23) Mulligan, F. L.; Babbini, D. C.; Davis, I. R.; Hurst, S. K.; Nichol, G. S. *Inorg. Chem.* **2009**, *48*, 2708–2710.
- (24) Babbini, D. C.; Cluff, K. J.; Fisher, N. B.; Charbonneau, J. C.; Nichol, G. S.; Hurst, S. K. *J. Organomet. Chem.* **2012**, *713*, 217–221.
- (25) Wade, C. R.; Lin, T. P.; Nelson, R. C.; Mader, E. A.; Miller, J. T.; Gabbai, F. P. *J. Am. Chem. Soc.* **2011**, *133*, 8948–8955.
- (26) (a) Zintl, E.; Harder, A. *Z. Phys. Chem., Abt. A* **1931**, *154*, 47–91. (b) Zintl, E.; Dullenkopf, W. *Z. Phys. Chem., Abt. B* **1932**, *16*, 183–194.
- (27) Hagelberg, F.; Das, T. P.; Weil, K. G. *J. Phys. Chem. A* **1998**, *102*, 4630–4637.
- (28) Goicoechea, J. M.; Hull, M. W.; Sevov, S. C. *J. Am. Chem. Soc.* **2007**, *129*, 7885–7893.
- (29) Frisch, M. J.; Trucks, G. W.; Schlegel, H. B.; Scuseria, G. E.; Robb, M. A.; Cheeseman, J. R.; Scalmani, G.; Barone, V.; Mennucci, B.; Petersson, G. A.; Nakatsuji, H.; Caricato, M.; Li, X.; Hratchian, H. P.; Izmaylov, A. F.; Bloino, J.; Zheng, G.; Sonnenberg, J. L.; Hada, M.; Ehara, M.; Toyota, K.; Fukuda, R.; Hasegawa, J.; Ishida, M.; Nakajima, T.; Honda, Y.; Kitao, O.; Nakai, H.; Vreven, T.; Montgomery, J. A., Jr.; Peralta, J. E.; Ogliaro, F.; Bearpark, M.; Heyd, J. J.; Brothers, E.; Kudin, K. N.; Staroverov, V. N.; Keith, T.; Kobayashi, R.; Normand, J.; Raghavachari, K.; Rendell, A.; Burant, J. C.; Iyengar, S. S.; Tomasi, J.; Cossi, M.; Rega, N.; Millam, J. M.; Klene, M. J.; Knox, E.; Cross, J. B.; Bakken, V.; Adamo, C.; Jaramillo, J.; Gomperts, R.; Stratmann, R. E.; Yazyev, O.; Austin, A. J.; Cammi, R.; Pomelli, C.; Ochterski, J. W.; Martin, R. L.; Morokuma, K.; Zakrzewski, V. G.; Voth, G. A.; Salvador, P.; Dannenberg, J. J.; Dapprich, S.; Daniels, A. D.; Farkas, O.; Foresman, J. B.; Ortiz, J. V.; Cioslowski, J.; Fox, D. J., *Gaussian 09*, Revision B.01; Gaussian, Inc.: Wallingford, CT, 2009.
- (30) Wade, K. *Adv. Inorg. Chem. Radiochem.* **1976**, *18*, 1–66.
- (31) Wiberg, K. B. *Tetrahedron* **1968**, *24*, 1083–1096.
- (32) Schmidbaur, H. *Gold Bulletin* **2000**, *33*, 3–10.
- (33) Pyykkö, P. *Angew. Chem., Int. Ed.* **2004**, *43*, 4412–4456.
- (34) Schmidbaur, H.; Schier, A. *Chem. Soc. Rev.* **2008**, *37*, 1931–1951.
- (35) Sculfort, S.; Braunstein, P. *Chem. Soc. Rev.* **2011**, *40*, 2741–2760.
- (36) Pyykkö, P.; Atsumi, M. *Chem. - Eur. J.* **2009**, *15*, 12770–12779.
- (37) Pyykkö, P. *J. Phys. Chem. A* **2015**, *119*, 2326–2337.
- (38) Dennington, R.; Keith, T.; Millam, J. *GaussView*, Version 5; Semichem Inc.: Shawnee Mission, KS, 2009.
- (39) Parr, R. G.; Pearson, R. G. *J. Am. Chem. Soc.* **1983**, *105*, 7512–7516.
- (40) Dapprich, S.; Frenking, G. *J. Phys. Chem.* **1995**, *99*, 9352–9362.
- (41) As pointed out in the text, the  $[Sb_3Au_3Sb_3]^{3-}$  cluster is a system with 24 valence electrons (Au d<sup>10</sup> and Sb 5s lone-pairs not counted). Of the 15 MOs depicted in Figure 2, the three in Figure 2A are a portion of the six Sb 5s lone-pairs, whereas the six in Figure 2C are six of the Au 5d lone-pairs, at the zeroth order. Thus, only the six MOs in Figures 2B,D belong to the 24 electron counting in  $[Sb_3Au_3Sb_3]^{3-}$ . The MOs for the remaining 12 valence electrons are responsible for six Sb–Sb  $\sigma$  single bonds, which are not shown in Figure 2.
- (42) Baird, N. C. *J. Am. Chem. Soc.* **1972**, *94*, 4941–4948.
- (43) While aromaticity is steadily conquering new territories beyond classical aromatic hydrocarbon molecules, some have remained cautious about the concept and only consider it a word.<sup>44</sup> However, aromatic Sb clusters are known in synthetic compounds such as  $Sb_4^{2-}$ .<sup>45</sup> Thus, we believe it is appropriate to claim  $[Sb_3Au_3Sb_3]^{3-}$  as an aromatic cluster, in particular in the context of the sandwich complexes.
- (44) Hoffmann, R. *Am. Sci.* **2015**, *103*, 18–22.
- (45) Critchlow, S. C.; Corbett, J. D. *Inorg. Chem.* **1984**, *23*, 770–774.
- (46) Schleyer, P. v. R.; Maerker, C.; Dransfeld, A.; Jiao, H.; Hommes, N. J. R. v. E. *J. Am. Chem. Soc.* **1996**, *118*, 6317–6318.
- (47) Chen, Z. F.; Wannere, C. S.; Corminboeuf, C.; Puchta, R.; Schleyer, P. v. R. *Chem. Rev.* **2005**, *105*, 3842–3888.